Graph-based model optimization of wind instruments: preliminary results

G. Le Vey[a] and J.F. Petiot[b]

[a]Ecole des Mines de Nantes, IRCCyN - UMR CNRS 6597, 4 rue Alfred Kastler, 44300 Nantes, France

[b]Ecole Centrale de Nantes, IRCCyN, 1 rue de la noe, 44321 Nantes, France

georges.le-vey@mines-nantes.fr

Recently, a graph-based modeling approach of wind instruments has been proposed [1] with the aim of computing natural frequencies in a way different from the usual impedance/transmission lines-based way. It can be easily applied, even to 2D or 3D networks of waveguides, under the assumption of 1D propagation, having complex geometries with branchings and discontinuities, allowing to study in the same framework musical instruments with or without toneholes. One important feature of this new approach is that mode matching is automatically satisfied from the very beginning of the procedure. In another paper of this conference [2], simulation results validated the approach. Further investigations in the same line are presented in [12]. In the present work, this model is compared to the classical transmission line model, where the instrument is regarded as a series of cylindrical or conical sections. For simple geometries (e.g. a succession of 3 cylindrical parts), the inharmonicities of the resonance frequencies are compared. For the transmission line model, an optimization of the harmonicity is conducted to obtain optimal dimensions of the resonator. With the graph-based approach, "harmonic" resonators are calculated exactly with closed-form expressions. Even if the results show an agreement between the two methods, the graph-based method presents the interest to provide all the possible "harmonic resonators", which can constitute an interesting characteristics for example in a design optimization process, by targeting a search domain.

1 Introduction

The characterization of the acoustical properties of resonators according to their geometry is an interesting problem in musical acoustics. Several musical instruments, like brasses, clarinets, saxophones, have acoustical properties and then musical qualities that depend on the acoustical resonances of their "bore", the inner shape of the resonator [3]. The prediction of these qualities is very important for instrument makers.

Brass wind instruments are traditionally characterized by their acoustic impedance Z_e, the transfer function between the acoustic flow and the acoustic pressure. The input impedance is a very important property for the characterization of a resonator: it gives the magnitude of the acoustical response to a forced oscillation. The experience shows that the frequency of the notes played by an instrument is mainly governed by the corresponding resonance frequency of the bore, but also by upper resonances [4]. For intonation and stability considerations, the resonance of the resonator must be close to a harmonic series [5].

The synthesis of bore geometries can be achieved with optimization techniques. Gradient-based optimization or genetic algorithms can be implemented to minimize an optimization criteria, generally based on the inharmonicity of the resonances frequencies [6-7-8-9]. These optimizations are able to provide interesting horn profiles but they remain subjected to the problem of local minima and are very sensitive to the initial solution and to the choice of the control parameters of the algorithm.

The calculation of the input impedance can be achieved with the transmission line model [10-11], where the instrument is regarded as a series of cylindrical or conical sections. A new modeling approach, described in [1], uses a description of a wind instrument through its graph in order to compute the natural frequencies of the resonator.

The objective of this paper is to compare the results of these two models on very simple geometries, and to show their complementarities in determining geometries with "harmonic" resonances.

In section 2, a brief description of the two models used for the characterization of the resonances of the bore of a resonator is presented: the transmission line model, and the graph-based model. Section 3 is dedicated to the results on a simple geometry, made of 3 cylindrical parts. Conclusions and perspectives are drawn in section 4.

2 Determination of resonances frequencies of resonators

The bore considered in this study is made of 3 cylindrical parts of same length (L = 0,1m) (Figure 1), defined by their radii r_i, and cross section a_i ($a_i = \pi r_i^2$; i=1 to 3). The wave number is $k = 2\pi f/c$, c the sound velocity and f the frequency. It is useful to define $x = \cos kL$.

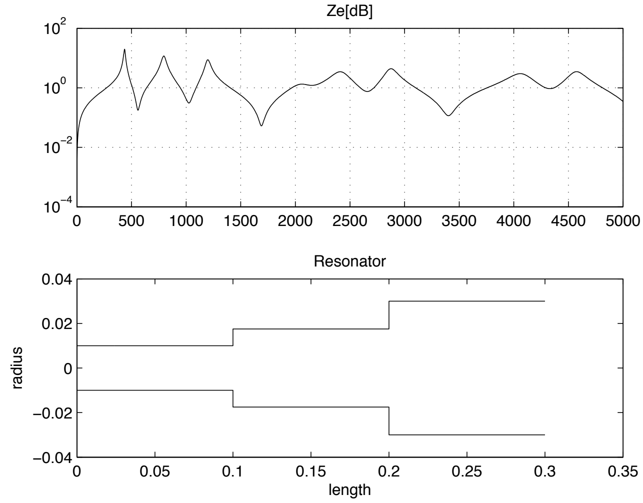

Figure 1: geometry of a resonator made of 3 cylinders, and the corresponding input impedance Ze (magnitude).

2.1 The TL-model: Input impedance calculations

The input impedance is a very important characteristic of a wind instrument. This quantity can be calculated or measured [10]. The calculation of the input impedance is traditionally made by a theoretical approach based on the transmission line modeling (TL-model) [10]. The model used for the computation of the input impedance Ze of wind instruments is the one-dimensional transmission line analogy, where the instrument is approximated by a series of truncated cones or cylinders [11] (linear acoustics, 1D, taking into account visco-thermal losses).

The resonance frequencies f_i of the resonator are given by an extraction of the maxima of the magnitude of the impedance (frequencies corresponding to the maximum of the module of Z_e).

2.2 Optimization of the resonator

Two objective functions *C1* and *C2* are proposed to represent the inharmonicity of the resonator: *C1* (Eq.1) is the squared error between the resonance frequencies ratio (relatively to the first resonance) and the nearest integer ratio:

$$C_1 = \sum_{i \in Rf} \left(\frac{f_i}{f_1} - i\right)^2 \qquad (1)$$

with *Rf*: set of integer ratio corresponding to the nearest integer $Rf = \left\{ i, / i = round(\frac{f_i}{f_1}) \right\}$; f_i: resonance frequency of the *i*-th impedance peak).

C2 (Eq.2) is the squared error between the resonance frequencies ratio (relatively to the first resonance) and a **predefined list** of integer ratio.

$$C_2 = \sum_{i \in PSf} \left(\frac{f_i}{f_1} - i\right)^2 \qquad (2)$$

with *PSf*: set of predefined integer ratios;.

To parameterize the optimization problem, the optimization variables x are the sections a_j of the j-th element. The optimization problem of the harmonicity can be stated as follows (Eq. 3):

$$x^* = \underset{x \in R^m}{\operatorname{argmin}} . C(X) \qquad (3)$$

In this paper, we consider only the two following cases with one optimization variable ($x=a_3$), or two variables ($x=(a_2, a_3)$). The value of a_1 has been fixed to $a_1 = 1$ cm^2 as only the ratio of the other cross-sections to it are meaningful. The optimization procedure has been programmed in *matlab* using the *fminsearch* function, a non-gradient based method that uses the simplex method starting at an initial estimate x_0. This algorithm gives only local minima but can handle discontinuities in the objective function.

2.3 The graph-based model

Recently [1], a modelling approach was introduced to compute efficiently the natural frequencies of wind instruments, possibly with toneholes, in the low frequency linear approximation. It is based on the description of these instruments through a graph, when looking at one instrument as a collection of 1D elementary components, which, at the present stage are cylinders, connected in some way. Then computing the natural frequencies of a wind instrument merely amounts to solving the laplacian on the corresponding graph that carries all the geometrical information (cross-sections, length). This is done thanks to a convenient encoding of the structure of the instrument into a matrix formulation and a special element by element matrix calculus, due to J. Hadamard (see [1] for details). Contrary to the usual method through the transmission lines formalism, the natural frequencies can be numerically computed as the solution of an algebraic eigenvalue problem, giving the eigenmodes –actually their value at the nodes of the graph- at the same time. Moreover, closed-form expressions are obtained for the equations to be satisfied by the natural frequencies and for the cross-sections themselves, at least for a low number of cylinders that constitute the resonator, as it is exposed in [2].

The special case of resonators without toneholes is investigated in a deeper way in the companion papers [2-12], to which we refer for the exposition of the method and various numerical results.

3 Results

The resonator considered in the study has a simple geometry made of 3 cylindrical parts of same length (figure 1). It is well known from the literature that a resonator made of cylindrical parts of same length with the section ratios given by $\frac{a_n}{a_1} = n.(n+1)/2$ gives an incomplete series of perfectly harmonic resonances (lossless case), the harmonics multiple of *n+1* being lacking: with 3 cylinders, the resonance ratios are in this case (1, 2, 3, 5, 6, 7, 9, 10, 11…) [13].

3.1 TL model: Calculation of the inharmonicity

With fixed values for a_1 and a_2 ($a_1 = 1$ cm^2, $a_2 = 3$ cm^2), the values of the criteria C_1 and C_2 were computed for different values of a_3. For the computation of C_2, the predefined set of resonance ratios *PSf* that have been considered are (1, 2, 3, 5, 6, 7, 9, 10).

The evolution of C_1 (resp. C_2) is given in Figure 2 (resp. in Figure 3).

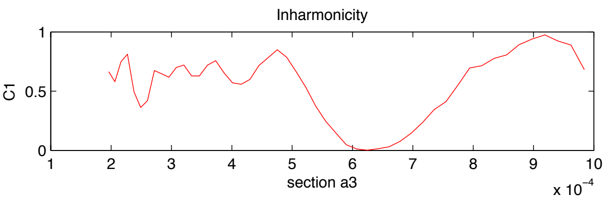

Figure 2: evolution of the criteria C_1 according to a_3 for a resonator made of 3 cylinders.

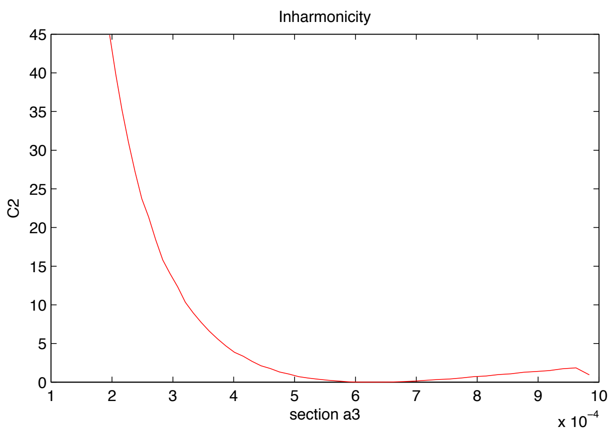

Figure 3: evolution of the criteria C_2 according to a_3 for a resonator made of 3 cylinders.

Whereas C_1 has many local minima, C_2 is strikingly convex. This is due to the fact that C_1 is not as constrained as C_2: with C_1, the solution has to fit on any integer frequency ratios, whereas it has to fit on a predefined list with C_2. As a consequence, an optimization process using C_2 will be much better conditioned than one with C_1. As expected, the results show that the resonator with $a_3 \simeq 6.2$

cm^2 (theoretically, without losses a_3/a_2 = 3*4/2=6) gets near zero values for the criteria C_1 or C_2, corresponding to perfectly harmonic resonances (1, 2, 3, 5, 6, 7, 9, 10) (given that losses are taken into account in the TL-model, the harmonic solution is not exactly equal to $a_3 = 6$ cm^2).

The results show also that only one particular value of a_3 allows a fitting of the resonances on the predefined ratios (1, 2, 3, 5, 6, 7, 9, 10). The criterion C_2 is convex in the domain of variation of a_3.

When the criterion considered is C_1, we can see on figure 2 that the inharmonicity is lower than for C_2, given that the resonances have to fit on the nearest integer ratio, not on a predefined list of ratios. But except the solution $a_3 \simeq 6.2$ cm^2, there is no other perfectly harmonic solution according to C_1 for the considered range of a_3.

With a fixed value for a_1 ($a_1 = 1$ cm^2), the values of the criteria C_1 and C_2 were computed for different values of (a_2, a_3). The evolution of C_1 (resp. C_2) is given in Figure 4 (resp. in Figure 5 and Figure 6, with a logarithmic scale).

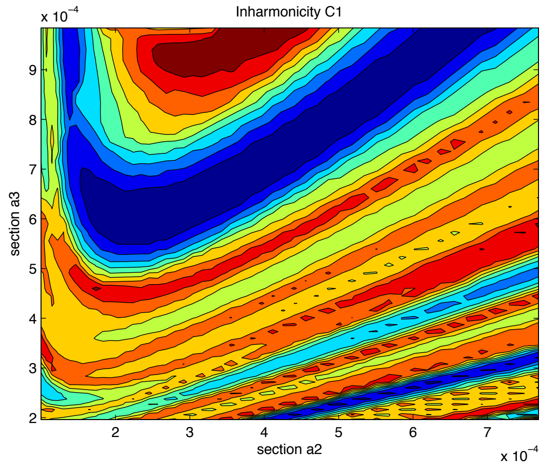

Figure 4: contour plot of the criteria C_1 according to (a_2, a_3) for a resonator made of 3 cylinders.

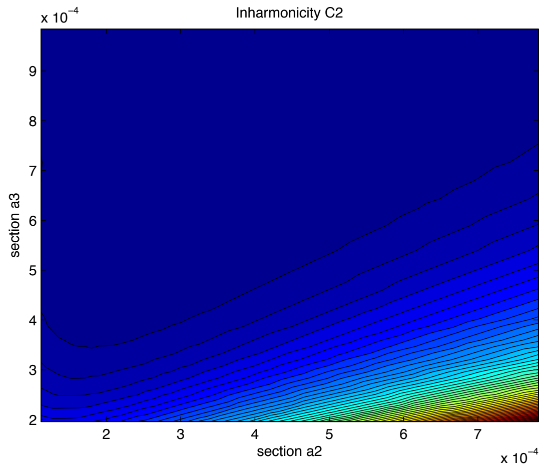

Figure 5: contour plot of the criteria C_2 according to (a_2, a_3) for a resonator made of 3 cylinders.

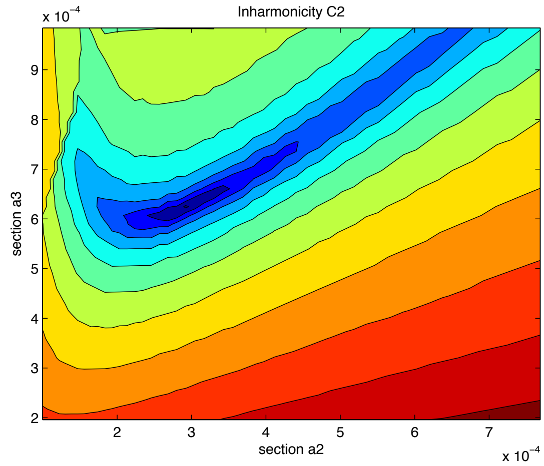

Figure 6: logarithmic contour plot of the criteria C_2 according to (a_2, a_3) for a resonator made of 3 cylinders.

Again, the resonator with $a_2 \simeq 3$ cm^2 and $a_3 \simeq 6$ cm^2 obtains perfectly harmonic resonances. But surprisingly, we observe on figure 4 that other combinations of values for a_2 and a_3 can produce almost harmonic resonances. For the criteria C_2, the response surface is very flat in the vicinity of the optimum. A logarithmic scale, represented figure 6, allows an easier visualization of the differences.

3.2 TL model: Optimization of the inharmonicity

In the case of the optimization of the inharmonicity according to a single variable, a_3, ($a_1 = 1$ cm^2, $a_2 = 3$ cm^2), the results given by the *fminsearch* function for the two objective C_1 and C_2 are presented in Table 1.

Table 1: results of the optimizations for one variable a_3.

Objective min.	Starting point x^0	Optimum x^*	Value of the criterion C(x*)
C_1	$a_3^0 = 3.14$	$a_3^{opt} = 3.41$	0.61
C_1	$a_3^0 = 4$	$a_3^{opt} = 4.14$	0.55
C_1	$a_3^0 = 5$	$a_3^{opt} = 6.29$	2e-3
C_2	$a_3^0 = 3.14$	$a_3^{opt} = 6.32$	1.19e-3
C_2	$a_3^0 = 4$	$a_3^{opt} = 6.32$	1.19e-3

For C_1, the results show that the optimum is strongly dependent on the starting point of the algorithm. This is due to the multiple local minima of C_1, presented in figure 2. Of course, more advances optimization strategies could be proposed to overcome this problem, but it will always remain a difficulty for large design space.

For C_2, the objective function being convex in the domain of study (figure 3), the convergence to the global minimum is insured whatever the starting point.

In the case of the optimization of the inharmonicity according to two variables, (a_2, a_3), ($a_1 = 1$ cm^2), the results are given in Table 2.

Table 2: results of the optimization for two variables (a_2, a_3).

Objective min.	Starting point x^0	Optimum x^*	Value of the criterion $C(x^*)$
C_1	$a_2^0 = 3.14$ $a_3^0 = 3.14$	$a_2^{opt} = 3.12$ $a_3^{opt} = 3.44$	0.61
C_1	$a_2^0 = 6$ $a_3^0 = 3$	$a_2^{opt} = 6.86$ $a_3^{opt} = 2.91$	0.077
C_1	$a_2^0 = 2.5$ $a_3^0 = 5$	$a_2^{opt} = 2.87$ $a_3^{opt} = 6.22$	1.9e-2
C_2	$a_2^0 = 3.14$ $a_3^0 = 3.14$	$a_2^{opt} = 2.89$ $a_3^{opt} = 6.23$	1.8e-3
C_2	$a_2^0 = 6$ $a_3^0 = 3$	$a_2^{opt} = 2.89$ $a_3^{opt} = 6.22$	1.8e-3
C_2	$a_2^0 = 2.5$ $a_3^0 = 5$	$a_2^{opt} = 2.71$ $a_3^{opt} = 6.09$	2.5e-3

For C_1, the results are strongly dependent on the starting point of the algorithm, due to the multiple local minima of C_1, presented in figure 4.

For C_2, the objective function being convex in the domain of study (figure 3), the convergence to the global minimum is insured whatever the starting point.

3.3 Graph-based model

Following the general methodology of [1], closed-form expressions for solving the problem of harmonically related natural frequencies of piecewise cylindrical resonators are presented in [2]. The main one is the nonlinear equation that these frequencies must satisfy. In [12], first numerical results based on these expressions are presented. For the sake of completeness, the expression for the case of a resonator with three cylinders is recalled here (Eq. 4):

$$x^2 = \frac{a_1 a_2 + a_1 a_3 + a_2^2}{(a_1 + a_2)(a_2 + a_3)} \tag{4}$$

from which we deduce the solution a_3 once the series of resonances is fixed through x (Eq 5.):

$$a_3 = \frac{a_2 (a_1 + a_2)(1 - x^2)}{(a_1 + a_2)x^2 - a_1} \tag{5}$$

Among these solutions, the only physically relevant are those satisfying (Eq. 6):

$$a_2 > \frac{a_1 (1 - x^2)}{x^2} \tag{6}$$

The relation between a_2 and a_3 for a harmonic resonator for the ratios (1, 2, 3, 5, 6, 7, 9, 10…) is given figure 3.

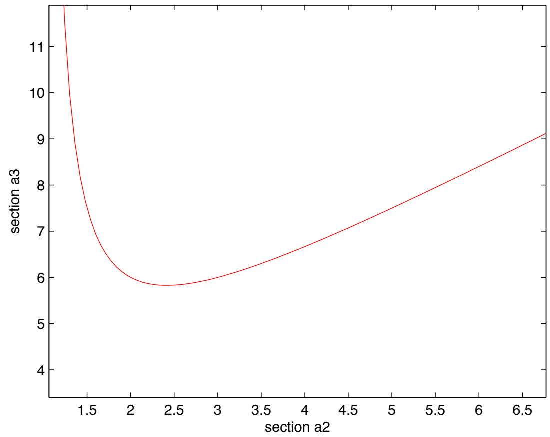

Figure 7: relation between a_2 and a_3 for harmonic resonances for the ratios (1, 2, 3, 5, 6, 7, 9, 10).

In figure 5, the curve of a_3 as a function of a_2, for $a_1 = 1$ and $kL = \pi/4$ is shown. Its behavior is typical of piecewise cylindrical resonators with three cylinders [12]. Notice the two integer solutions: { $a_2 = 3$, $a_3 = 6$} and { $a_2 = 2$, $a_3 = 6$} and the fact that there is a continuum of solutions: for $kL = \pi/4$ and for all the points { a_2, a_3} on this curve, one gets a harmonic resonator with the prespecified series kL of natural frequencies. For any choice of kL such that kL/π is a rational number, one will get with a similar curve a whole family of resonators with the prescribed series of harmonic resonances [12]. Thus one has a way to design precisely a bore for which a predetermined set of resonances are chosen and as a consequence to localize the good solutions for harmonic resonators for example in the design process of the bore through optimization. For example, some resonators can be much more sensitive to variations in the cross-sections than others, although they have the same series of resonances. Thus it is important to have a mean to characterize the robustness of the solutions.

A very important observation concerning figure 6 and 7 is that the shape of the minimal value of the criterion C_2 is in perfect agreement (up to the thermal losses) with the curve a_3 as a function of a_2 given by the graph method.

We notice finally that both methods give results that are in agreement and complementary:

- the TL-model gives the value of the criterion in the whole design space (a_2, a_3), in a numerical form (no closed-form of optimal solutions)
- the graph model limits to the perfectly harmonic designs, but gives the explicit relationship between the design variables

This simple situation where 2D graphs can be plotted allow us to check each approach against the other. In the more general case (more than 3 cylinders), as we cannot plot higher dimensional graphs, both methods can be used in conjunction. The graph method can be used to localize first where solutions should be searched after, in order to start an optimization process in a safer way.

6 Conclusion

In the design process of the bore of wind instruments, optimization methods often show numerous local maxima in the criterion to be optimized. This asks for constraining the optimization problem sufficiently. In the present work, one has seen that using a different modeling approach for the bore and its subsequent closed-form expressions, the starting point of involved iterative procedures can be targeted precisely. Whereas the graph-based modeling approach deals *stricto sensu* with exactly computing a piecewise cylindrical bore to have harmonically related natural frequencies, an optimization process is able to take into account many different constraints (ergonomics or manufacturing constraints on the bore) imposed by the design.

In that respect, parallel work has shown that the graph-based modeling approach seems able to furnish information about the sensitivity of some bore shapes, within a family of bores having a prescribed series of harmonic natural frequencies. The conjunction of both approaches opens perspectives concerning a robust regularization of the inharmonicity criterion. Thus their joint use can be valuable and is promising. This has to be investigated in a deeper way.

References

[1] G. Le Vey. Graph-based models for woodwinds. In SMAC2013, Stockholm Music Acoustics Conference, Stockholm, July 2013.

[2] G. Le Vey. Graph models of wind instruments: computing the natural frequencies of some elementary ducts. In ISMA 2014, Le Mans, France, July 2014. Submitted.

[3] Campbell M. Brass Instruments as we know them today. Acta acustica united with Acustica, Vol. 90, N°4 (2004), pp 600-610.

[4] Benade A.H., Gans D.J. 'Sound production in wind instruments'. *Ann. N.Y. Acad. Sci*. 155 pp. 247-263 (1968).

[5] Eveno P., Petiot J-F., Gilbert J., Kieffer B., Caussé R. The relationship between resonances frequencies and playing frequencies in trumpets. Acta Acustica united wih Acustica. 03/2014. Vol. 100(2), 362-374.

[6] Kausel W. Optimization of brasswind instruments and its application in bore reconstruction. *Journal of New Music Research*, 30, 69-82, 2001.

[7] E. Bängtsson, D. Noreland, and M. Berggren. Shape optimization of an acoustic horn. *Computer methods in applied mechanics and engineering*, 192(11-12):1533–1571, 2003.

[8] Poirson E., Petiot J-F., Gilbert G. Integration of user-perceptions in the design process: application to musical instrument optimisation. *Journal of Mechanical Design*, Vol.129, No.12, December 2007, pp1206-1214.

[9] J-F. Petiot and F. Tavard. Design and manufacturing of an artificial marine conch by bore optimisation. In Acoustics 2008, Paris, France, June, July 2008.

[10] Dalmont J-P., Bruneau A.M. 'Acoustic impedance measurement : plane wave mode and first helical mode contributions' *J. Acoust. Soc. Am*. 91 pp. 3026-3033 (1991).

[11] Caussé R., Kergomard J., Lurton X. Input impedance of brass musical instruments, comparison between experiment and numerical models. J. Acoust. Soc. Am. 75, 241-254 (1984).

[12] J.P. Dalmont, G. Le Vey, « New lattices of sound tubes with harmonically related frequencies », ISMA 2014, Le Mans, July 2014.

[13] J. P. Dalmont and J. Kergomard. Lattices of sound tubes with harmonically related eigenfrequencies. Acta Acustica, 2(5):421–430, 1994.